A fully coupled diffusional-mechanical formulation: numerical implementation, analytical validation, and effects of plasticity on equilibrium

A. Villani, E. P. Busso, K. Ammar, S. Forest & M. G. D. Geers

☘ Springer

Springer

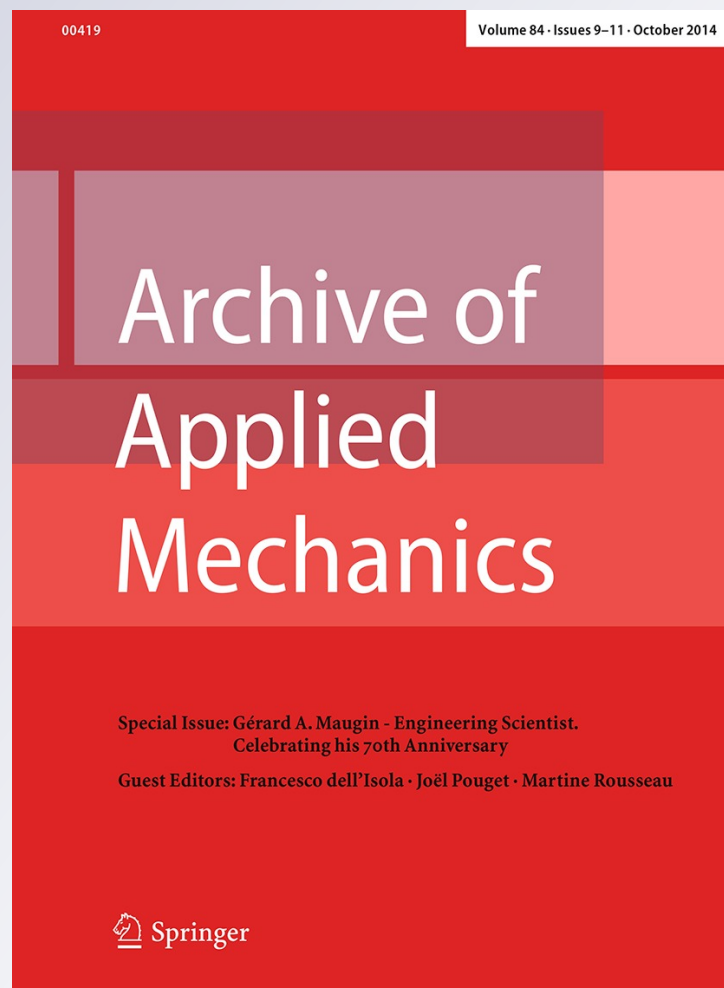**SPECIAL ISSUE**

A. Villani · E. P. Busso · K. Ammar · S. Forest ·
M. G. D. Geers

A fully coupled diffusional-mechanical formulation: numerical implementation, analytical validation, and effects of plasticity on equilibrium

Abstract A macroscopic coupled stress-diffusion theory which accounts for the effects of nonlinear material behaviour, based on the framework proposed by Cahn and Larché, is presented and implemented numerically into the finite element method. The numerical implementation is validated against analytical solutions for different boundary valued problems. Particular attention is payed to the open system elastic constants, i.e. those derived at constant diffusion potential, since they enable, under circumstances, the equilibrium composition field for any generic chemical-mechanical coupled problem to be obtained through the solution of an equivalent elastic problem. Finally, the effects of plasticity on the overall equilibrium state of the coupled problem solution are discussed.

1 Introduction

Problems involving diffusion in a stressed material system can be found in numerous applications generally concerned with high homologous temperatures, such as thin films in semiconductor devices and power plant and aero-engine components. The transport of matter by diffusion under stress can generally result in the gradual degradation of the material microstructure, leading to the nucleation of local damage (e.g. stable vacancy clusters or micro-voids, micro-cracks). The presence of such local damage events could impede the correct performance of the component or device and limit its targeted service life. It is thus critical to model accurately the motion of diffusing species and point defects in complex material systems operating under severe loading and environmental conditions.

Podstrigach and coworkers [17] were the first to develop a thermodynamic theory of stress-diffusion coupling. It relies on the choice of a specific free energy function, and analytical solutions in the case of elastic mechanical behaviour are provided for a loaded plate with a hole [18] and the bending of a plate

A. Villani, K. Ammar, S. Forest (✉)
UMR CNRS 7633, Centre des Matériaux, MINES ParisTech, BP. 87, 91003 Evry Cedex, France
Tel.: +33 1 60 76 30 69
E-mail: Samuel.forest@ensmp.fr

E. P. Busso
ONERA, B.P. 80100, 91123 Palaiseau cedex, France
E-mail: esteban.busso@onera.fr

A. Villani
E-mail: aurelien.villani@ensmp.fr

M. G. D. Geers
Mechanical Engineering, Eindhoven University of Technology, PO Box 513, 5600 MB Eindhoven, The Netherlands

[16]. Cahn and Larché [6] further developed this coupled stress-diffusion theory and introduced the concept of open system elastic moduli. In their thermodynamic theory (see [7] for full details, and [3] for a broad discussion), the convenient concept of network is introduced, whereby all atoms are assumed to be capable of diffusing. In a crystal, for instance, the lattice itself can be assumed to act as the network and to remain coherent. Equilibrium can then be attained by considering a constant and homogeneous diffusion potential. Cahn and Larché introduced the concept of open system elastic constants, or elastic constants derived at constant diffusion potential, in order to obtain a linearised version of the nonlinear coupled problem. Maugin [13] also addressed extensively the thermodynamic problem of a diffusive variable, without stress coupling, albeit considering the first gradient of the concentration as well.

Other approaches have been used to model specific problems involving the coupling between stress and diffusion. For instance, the diffusion of vacancies within the heterogeneous stress field around an edge dislocation core has been treated in [19] using Bessel functions. In contrast, boundary value problems involving coupled diffusion-stress phenomena have been solved analytically using Cosserat spectrum theory in [15]. In [24] and [25], finite element solutions involving stress-induced diffusion in a plate subject to different types of boundary conditions were reported. In [22], the authors relied on Lambert functions to derive an analytical solution of the chemical concentration in a loaded rod, and compared it to a coupled finite element formulation. Finally, Anand [2] developed a thermodynamical theory which accounts for diffusion of hydrogen and heat coupled with the mechanical problem.

The theory is implemented numerically using the finite element method and used to solve three elastic and elasto-plastic stress-diffusion boundary value problems, out of which two were never addressed in the literature before. The first one involves a coupled diffusion-stress formulation for a disc rotating at high speeds and temperature, i.e. at conditions similar to those encountered in gas turbine engine components. The second concerns the classical redistribution of vacancies around an edge dislocation, as described in [11], which can be related to a recent paper by Cahn [5]. Finally, a problem relevant to vacancy diffusion-driven cavitation in nuclear reactor components is studied, i.e. the redistribution of vacancies in a loaded perforated plate, influenced by plasticity.

The objective of the present paper is to provide a validation of the fully coupled implementation against the systematic analytical solution given by Cahn and Larché, complemented by the introduction of internal variables necessary to address plasticity. The introduction of plasticity in the constitutive equations allows for a direct extension of the general solution of Cahn and Larché, for a given plastic strain field. In addition, the coupled elastoviscoplastic diffusion theory is formulated and implemented by means of the finite element method in order to simulate true evolution problems.

Standard tensorial notation will be used throughout the paper. Unless otherwise specified, vectors will be described by boldface lower case letters, second order tensors by boldface upper case letters, and fourth order tensors by italic upper case letters. The formulation is limited to the small strain isothermal case for which analytical solutions can be derived.

2 Continuum thermodynamic coupled diffusion-stress theory

2.1 Balance equations

The diffusing species are assumed to be solute atoms and vacancies. The vacancy concentration obeys the mass balance equation, which relates the concentration, c, to the flux vector, $\mathbf{j}$,

$$
\begin{aligned}
\dot{c} &= -\mathrm{div}\,\mathbf{j} \text{ on } V \\
j &= \mathbf{j} \cdot \mathbf{n} \text{ on } \partial V
\end{aligned}
\tag{1}
$$

where no source term is considered. The concentration is defined as the ratio between the lattice sites occupied by solute atoms or vacancies and the total number of lattice sites in the material point of the crystalline solid. The mechanical static equilibrium is defined by:

$$
\begin{aligned}
\mathrm{div}\,\boldsymbol{\sigma} + \mathbf{f} &= 0 \text{ on } V \\
\mathbf{t} &= \boldsymbol{\sigma} \cdot \mathbf{n} \text{ on } \partial V
\end{aligned}
\tag{2}
$$

where $\boldsymbol{\sigma}$ is the stress tensor, $\mathbf{f}$ is the body force vector in V and $\mathbf{t}$ the traction vector acting on ∂V.

2.2 Constitutive equations

2.2.1 General theory

The total strain is partitioned as:

$$\epsilon = \epsilon^{\mathrm{e}} + \epsilon^{\mathrm{p}} + \epsilon^{\star}(c) \tag{3}$$

where ϵ^{e} is the elastic strain tensor, ϵ^{p} the plastic strain tensor, and $\epsilon^{\star}$ the eigenstrain tensor, representing the volume change associated with the substitution of species in lattice sites. The latter typically depends on the concentration, c, as

$$\epsilon^{\star}(c) = (c - c_{\mathrm{ref}})\, \mathbf{H} + \epsilon^{\star}_{\mathrm{ref}}. \tag{4}$$

Here, $\epsilon^{\star}_{ref}$ is the eigenstrain tensor corresponding to the reference concentration, c_{ref}, and the tensor $\mathbf{H} = \dfrac{\partial \epsilon}{\partial c}$ scales the concentration change. Recall the first law of thermodynamics:

$$\int_V \dot{e}\,\mathrm{d}V = \int_V \boldsymbol{\sigma} : \dot{\epsilon}\,\mathrm{d}V \tag{5}$$

where, e, is the internal energy density per unit volume and $\boldsymbol{\sigma}$ the stress tensor. The second law states that:

$$\int_V \dot{s}\,\mathrm{d}V - \int_{\partial V} \frac{\mu \mathbf{j}}{T} \cdot \mathbf{n}\,\mathrm{d}S \geq 0 \tag{6}$$

where, s, is the entropy density, T, the absolute temperature, and μ the diffusion potential.[1] The local form of the second law (6), for a constant and uniform temperature field, reads:

$$T\dot{s} - \mathrm{div}\,(\mu \mathbf{j}) \geq 0 \tag{7}$$

Recalling $\psi = e - Ts$, the free energy density per unit volume at constant temperature, then Eq. (7) yields the local form of the dissipation inequality:

$$\mathcal{D} = \boldsymbol{\sigma} : \dot{\epsilon} - \mathrm{div}\,(\mu \mathbf{j}) - \dot{\psi} \geq 0 \tag{8}$$

The diffusion-stress coupling is introduced in the choice of the free energy volumetric density function. Here, it is assumed to consist of a mechanical and a chemical part, which depend on several independent state variables, i.e. the elastic strain tensor ϵ^{e}, an isotropic scalar hardening variable r, a traceless kinematic tensorial hardening variable, $\boldsymbol{\alpha}$ [12], and the vacancy concentration, c. Then,

$$\psi(\epsilon^{\mathrm{e}}, r, \boldsymbol{\alpha}, c) = \psi^{\mathrm{mech}}(\epsilon^{\mathrm{e}}, r, \boldsymbol{\alpha}, c) + \psi^{\mathrm{chem}}(c). \tag{9}$$

The mechanical part of the free energy is defined as,

$$\psi^{\mathrm{mech}}(\epsilon^{\mathrm{e}}, r, \boldsymbol{\alpha}, c) = \frac{1}{2}\epsilon^{\mathrm{e}} : \mathcal{C}(c) : \epsilon^{\mathrm{e}} + \psi^{\mathrm{mech,p}}(r, \boldsymbol{\alpha}, c), \tag{10}$$

where $\mathcal{C}$ is elastic moduli fourth order tensor, and $\psi^{\mathrm{mech,p}}(r, \boldsymbol{\alpha}, c)$ corresponds to the energy stored by work-hardening. The dissipation can then be expressed in terms of Eqs. (8), (1) and (9) as:

$$\mathcal{D} = \left(\boldsymbol{\sigma} - \frac{\partial \psi}{\partial \epsilon^{\mathrm{e}}}\right) : \dot{\epsilon}^{\mathrm{e}} + \left(\mu + \boldsymbol{\sigma} : \mathbf{H} - \frac{\partial \psi}{\partial c}\right)\dot{c} - \mathbf{j} \cdot \nabla \mu + \boldsymbol{\sigma} : \dot{\epsilon}^{\mathrm{p}} - \frac{\partial \psi}{\partial r}\dot{r} - \frac{\partial \psi}{\partial \boldsymbol{\alpha}} : \dot{\boldsymbol{\alpha}} \geq 0 \tag{11}$$

The condition (11) depends linearly on the independent variables $\dot{\epsilon}^{\mathrm{e}}$, $\dot{c}$, and the terms in brackets are independent of $\dot{\epsilon}^{\mathrm{e}}$ and $\dot{c}$. The state laws then follow for the stress and diffusion potential (using Coleman-Noll argument):

$$\boldsymbol{\sigma} = \frac{\partial \psi}{\partial \epsilon^{\mathrm{e}}}, \tag{12}$$

---

[1] In the sense of Cahn and Larché: $\mu = \mu^{\mathrm{s}} - \mu^{\mathrm{h}}$, where μ^{s} is the chemical potential of the species under consideration, and μ^h is the chemical potential of the host atoms.

$$\mu = \frac{\partial \psi}{\partial c} - \boldsymbol{\sigma} : \mathbf{H}, \tag{13}$$

The following thermodynamic forces can be inferred from Eq. (11),

$$R_{\mathrm{p}} = \frac{\partial \psi}{\partial r}, \quad \mathbf{X} = \frac{\partial \psi}{\partial \boldsymbol{\alpha}} \tag{14}$$

The dissipation inequality then simplifies to:

$$-\mathbf{j} \cdot \nabla \mu + \boldsymbol{\sigma} : \dot{\boldsymbol{\epsilon}}^{\mathrm{p}} - R_{\mathrm{p}} \dot{r} - \mathbf{X} : \dot{\boldsymbol{\alpha}} \geq 0 \tag{15}$$

To ensure positiveness of the dissipation, the existence of a convex dissipation potential $\Omega(\boldsymbol{\sigma}, R_{\mathrm{p}}, \mathbf{X}, \nabla \mu)$, is assumed so that :

$$\dot{r} = -\frac{\partial \Omega}{\partial R_{\mathrm{p}}}, \quad \dot{\boldsymbol{\alpha}} = -\frac{\partial \Omega}{\partial \mathbf{X}}, \quad \dot{\boldsymbol{\epsilon}}^{\mathrm{p}} = \frac{\partial \Omega}{\partial \boldsymbol{\sigma}}, \quad \mathbf{j} = -\frac{\partial \Omega}{\partial \nabla \mu} \tag{16}$$

In the case of rate-independent plasticity, which is of practical interest here for enabling analytical solutions, two distinct potentials, Ω^{mech} and Ω^{chem}, are introduced such that

$$\dot{r} = -\dot{\lambda} \frac{\partial \Omega^{\mathrm{mech}}}{\partial R_{\mathrm{p}}}, \quad \dot{\boldsymbol{\alpha}} = -\dot{\lambda} \frac{\partial \Omega^{\mathrm{mech}}}{\partial \mathbf{X}}, \quad \dot{\boldsymbol{\epsilon}}^{\mathrm{p}} = \dot{\lambda} \frac{\partial \Omega^{\mathrm{mech}}}{\partial \boldsymbol{\sigma}}, \quad \mathbf{j} = -\frac{\partial \Omega^{\mathrm{chem}}}{\partial \nabla \mu} \tag{17}$$

where $\dot{\lambda}$ is the plastic multiplier. A yield function, $g(\boldsymbol{\sigma}, \mathbf{X}, R_{\mathrm{p}})$, can be defined so that $\dot{\lambda} g = 0, \dot{\lambda} \geq 0, g \leq 0$. The consistency condition under plastic loading reads:

$$\dot{g} = 0 = \frac{\partial g}{\partial \boldsymbol{\sigma}} : \dot{\boldsymbol{\sigma}} + \frac{\partial g}{\partial \mathbf{X}} : \dot{\mathbf{X}} + \frac{\partial g}{\partial R_{\mathrm{p}}} \dot{R}_{\mathrm{p}}, \tag{18}$$

from which the plastic multiplier is obtained,

$$\dot{\lambda} = \frac{\dfrac{\partial g}{\partial \boldsymbol{\sigma}} : \dfrac{\partial^2 \psi}{\partial \boldsymbol{\epsilon}^{\mathrm{e}2}} : \dot{\boldsymbol{\epsilon}} + \left(\dfrac{\partial g}{\partial \boldsymbol{\sigma}} : \dfrac{\partial^2 \psi}{\partial \boldsymbol{\epsilon}^{\mathrm{e}} \partial c} \right) \dot{c}}{\dfrac{\partial g}{\partial \boldsymbol{\sigma}} : \dfrac{\partial^2 \psi}{\partial \boldsymbol{\epsilon}^{\mathrm{e}2}} : \dfrac{\partial \Omega^{\mathrm{mech}}}{\partial \boldsymbol{\sigma}} + \dfrac{\partial g}{\partial R_{\mathrm{p}}} \dfrac{\partial^2 \psi}{\partial r^2} \dfrac{\partial \Omega^{\mathrm{mech}}}{\partial R_{\mathrm{p}}} + \dfrac{\partial g}{\partial \mathbf{X}} : \dfrac{\partial^2 \psi}{\partial \boldsymbol{\alpha}^2} : \dfrac{\partial \Omega^{\mathrm{mech}}}{\partial \mathbf{X}}}. \tag{19}$$

In the Eq. (19), $\psi^{\mathrm{mech,p}}$ is assumed to be independent of c.

2.2.2 Choice of potential and energy functions

The chemical free energy component in Eq. (9) is expressed in a standard form [9]:

$$\psi^{\mathrm{chem}}(c) = \frac{E_f c}{v_a} + \frac{R T}{v_a} \left(c \ln(c) + (1-c) \ln(1-c) \right), \tag{20}$$

where, E_f, is the formation enthalpy of a mole of the considered species, T, is the absolute temperature and, R, is the universal gas constant. The tensor $\mathbf{H}$ takes the form $\mathbf{H} = \eta \mathbf{1}$ for the particular case of isotropy, where $\mathbf{1}$ is the second order identity tensor and

$$\eta = \frac{1}{3} \frac{\Delta v}{v_a}. \tag{21}$$

In the above equation, Δv, is the relaxed lattice volume after one mole of atoms is removed from the lattice, and v_a, the volume occupied by a mole of atoms. Equation (4) then becomes,

$$\boldsymbol{\epsilon}^{\star}(c) = \eta(c - c_{\mathrm{ref}}) \mathbf{1} + \boldsymbol{\epsilon}_{\mathrm{ref}}^{\star}. \tag{22}$$

Finally, the diffusion potential is expressed as:

$$\mu = \frac{\partial \psi}{\partial c} - \boldsymbol{\sigma} : \mathbf{H} = \frac{RT}{v_a} \left(\ln \left(\frac{c}{1-c} \right) + \frac{E_f}{RT} \right) - \eta \operatorname{tr}(\boldsymbol{\sigma}). \tag{23}$$

Following [12], the plastic term in the free energy (10) is taken as:

$$\psi^{\text{mech,p}} = R_\infty \left(r + \frac{1}{b}[\exp(-br) - 1] \right) + \frac{1}{3}C\boldsymbol{\alpha} : \boldsymbol{\alpha} \tag{24}$$

where R_∞, b and C are material parameters. The thermodynamic forces are expressed from Eq. (14) as:

$$\begin{aligned}
R_{\text{p}} &= \frac{\partial \psi}{\partial r} = R_\infty \left(1 - \exp(-br) \right), \\
\mathbf{X} &= \frac{\partial \psi}{\partial \boldsymbol{\alpha}} = \frac{2}{3}C\boldsymbol{\alpha}.
\end{aligned} \tag{25}$$

The yield function, $g(\boldsymbol{\sigma}, \mathbf{X}, R_{\text{p}})$, is defined by:

$$g(\boldsymbol{\sigma}, \mathbf{X}, R_{\text{p}}) = \sigma_{\text{eq}} - R_{\text{p}} - \sigma_y, \tag{26}$$

where σ_y is the initial yield strength, σ_{eq} is the effective equivalent stress, defined as:

$$J_2(\boldsymbol{\sigma} - \mathbf{X}) = \sqrt{\frac{3}{2}(\boldsymbol{\sigma}^{\text{dev}} - \mathbf{X}^{\text{dev}}) : (\boldsymbol{\sigma}^{\text{dev}} - \mathbf{X}^{\text{dev}})} \tag{27}$$

$\boldsymbol{\sigma}^{\text{dev}}$ and $\mathbf{X}^{\text{dev}}$ are defined as the deviators of $\boldsymbol{\sigma}$ and $\mathbf{X}$, respectively.

For time-dependent plasticity, the dissipation potential is taken to be:

$$\Omega(R_{\text{p}}, \boldsymbol{\sigma}, \nabla\mu) = \frac{K_a}{n+1} \left\langle \frac{g(\boldsymbol{\sigma}, \mathbf{X}, R_{\text{p}})}{K_a} \right\rangle^{n+1} + \frac{1}{2}\mathbf{L}(c) : \nabla\mu \otimes \nabla\mu \tag{28}$$

where K_a and n are material parameters. The term $\langle a \rangle = a$ if $a > 0$, else $\langle a \rangle = 0$.

Using the functions introduced in this section, Eq. (16) becomes :

$$\begin{aligned}
\dot{r} &= -\frac{\partial \Omega}{\partial R_{\text{p}}} = \left\langle \frac{\sigma_{\text{eq}} - R_{\text{p}} - \sigma_y}{K_a} \right\rangle^n \\
\dot{\boldsymbol{\epsilon}}^{\text{p}} &= \frac{\partial \Omega}{\partial \boldsymbol{\sigma}} = \frac{\partial \Omega}{\partial \sigma_{\text{eq}}} \frac{\partial \sigma_{\text{eq}}}{\partial \boldsymbol{\sigma}} = \frac{3}{2} \left\langle \frac{\sigma_{\text{eq}} - R_{\text{p}} - \sigma_y}{K_a} \right\rangle^n \frac{\boldsymbol{\sigma}^{\text{dev}} - \mathbf{X}^{\text{dev}}}{\sigma_{\text{eq}}} \\
\dot{\boldsymbol{\alpha}} &= -\frac{\partial \Omega}{\partial \mathbf{X}} = -\frac{\partial \Omega}{\partial \sigma_{\text{eq}}} \frac{\partial \sigma_{\text{eq}}}{\partial \mathbf{X}} = \frac{3}{2} \left\langle \frac{\sigma_{\text{eq}} - R_{\text{p}} - \sigma_y}{K_a} \right\rangle^n \frac{\boldsymbol{\sigma}^{\text{dev}} - \mathbf{X}^{\text{dev}}}{\sigma_{\text{eq}}} = \dot{\boldsymbol{\epsilon}}^{\text{p}}
\end{aligned} \tag{29}$$

For time-independent plasticity, the dissipation potentials considered reads [12]:

$$\Omega^{\text{mech}} = g(\boldsymbol{\sigma}, \mathbf{X}, R_{\text{p}}), \quad \Omega^{\text{chem}} = \frac{1}{2}\mathbf{L}(c) : \nabla\mu \otimes \nabla\mu, \tag{30}$$

The evolution of the plastic internal variable given by Eq. (17) becomes:

$$\begin{aligned}
\dot{r} &= -\dot{\lambda}\frac{\partial \Omega^{\text{mech}}}{\partial R_{\text{p}}} = \dot{\lambda} \\
\dot{\boldsymbol{\epsilon}}^{\text{p}} &= \dot{\lambda}\frac{\partial \Omega^{\text{mech}}}{\partial \boldsymbol{\sigma}} = \dot{\lambda}\frac{3}{2}\frac{\boldsymbol{\sigma}^{\text{dev}} - \mathbf{X}^{\text{dev}}}{\sigma_{\text{eq}}} \\
\dot{\boldsymbol{\alpha}} &= -\dot{\lambda}\frac{\partial \Omega^{\text{mech}}}{\partial \mathbf{X}} = \dot{\lambda}\frac{3}{2}\frac{\boldsymbol{\sigma}^{\text{dev}} - \mathbf{X}^{\text{dev}}}{\sigma_{\text{eq}}} = \dot{\boldsymbol{\epsilon}}^{\text{p}}
\end{aligned} \tag{31}$$

It is assumed that, for the isotropic case,

$$\mathbf{L}(c) = L(c)\mathbf{1} = \frac{D v_a}{RT}c(1 - c)\mathbf{1}, \tag{32}$$

with D being the diffusivity. Then, substitution of Eq. (32) and the gradient of Eq. (23) into Eq. (17) leaves,

$$\mathbf{j} = -D\nabla c + \frac{1}{3}\frac{D\Delta v}{RT}c(1-c)\nabla(\mathrm{tr}(\boldsymbol{\sigma})) \tag{33}$$

Equation (33) clearly reveals the two main driving forces controlling the vacancy flux: the concentration gradient term arising from inhomogeneities in the composition, and the mechanical contribution via the stress gradient.

2.3 Equilibrium composition field

2.3.1 Theory

In this part, it will be shown that, provided that an elastic solution of the purely mechanical problem is known, an equilibrium composition field can be obtained taking the two-way coupling into account. The plastic deformation field, $\boldsymbol{\epsilon}^{\mathrm{p}}$, will be assumed to be known in the whole body and to be constant.

At equilibrium, the diffusion potential is constant and satisfies the mass balance Eq. (1). Following the work of Cahn and Larché [7], the composition c is a function of stress alone. An expression for the equilibrium chemical concentration is obtained in terms of the corresponding diffusion potential, μ_{eq}, from Eq. (23) assuming that $c \ll 1$. For the fully anisotropic case (where $\mathbf{H} \neq \eta\mathbf{1}$):

$$c_{\mathrm{eq}} = \exp\left(\frac{v_a}{RT}\mu_{\mathrm{eq}} - \frac{E_f}{RT}\right)\exp\left(\frac{v_a}{RT}\mathbf{H}:\boldsymbol{\sigma}\right). \tag{34}$$

Let us define

$$\left.\frac{\partial\mu}{\partial c}\right|_{\sigma_{ij}=0} = \frac{1}{\chi}, \tag{35}$$

Using (23) and (35) for small values of c implies that

$$\chi = \frac{v_a}{RT}c \tag{36}$$

Denoting $c_0 = \exp\left(\frac{v_a}{RT}\mu_{\mathrm{eq}} - \frac{E_f}{RT}\right)$, the composition field is linearised in the form given by [7]:

$$c_{\mathrm{eq}} = c_0 + \chi\mathbf{H}:\boldsymbol{\sigma} \tag{37}$$

where χ has been evaluated for $c = c_0$. Using (37) in (4), at equilibrium:

$$\begin{aligned}
\boldsymbol{\epsilon}^{\star} &= (c_{\mathrm{eq}} - c_{\mathrm{ref}})\mathbf{H} + \boldsymbol{\epsilon}^{\star}_{\mathrm{ref}} \\
&= (c_0 - c_{\mathrm{ref}})\mathbf{H} + \chi\mathbf{H}\otimes\mathbf{H}:\boldsymbol{\sigma} + \boldsymbol{\epsilon}^{\star}_{\mathrm{ref}}
\end{aligned} \tag{38}$$

According to Hooke's law, $\boldsymbol{\sigma} = \mathcal{C}:(\boldsymbol{\epsilon} - \boldsymbol{\epsilon}^{\star}(c) - \boldsymbol{\epsilon}^{\mathrm{p}})$, and using (38), the total strain tensor can be expressed as,

$$\boldsymbol{\epsilon} = (\mathcal{S} + \chi\mathbf{H}\otimes\mathbf{H}):\boldsymbol{\sigma} + \boldsymbol{\epsilon}^{\mathrm{p}} + \boldsymbol{\epsilon}^{\star}_{\mathrm{ref}} + (c_0 - c_{\mathrm{ref}})\mathbf{H} \tag{39}$$

where $\mathcal{S} = \mathcal{C}^{-1}$. In the above equation, the term in parentheses is called the open system compliance[2] by Cahn and Larché [7]:

$$\mathcal{S}^0_{ijkl} = S_{ijkl} + \chi H_{ij}H_{kl}. \tag{40}$$

The remaining equation to be solved is the mechanical balance equation, which now takes the form:

$$\mathrm{div}\,\boldsymbol{\sigma} + \mathbf{f} = \mathrm{div}\left(\mathcal{S}_0^{-1}(\boldsymbol{\epsilon} - \boldsymbol{\epsilon}^{\mathrm{p}} - \boldsymbol{\epsilon}^{\star}_{\mathrm{ref}} - (c_0 - c_{\mathrm{ref}})\mathbf{H})\right) + \mathbf{f} = \mathbf{0} \tag{41}$$

The equilibrium mechanical-diffusion problem is now equivalent to solving the purely elastic problem (41) for a given fictitious compliance field, $\mathcal{S}_0$.

---

[2] They are derived at constant diffusion potential, as shown in "Appendix 5."

For an elastic isotropic material, the compliance components are

$$\mathcal{S}_{ijkl} = -\frac{\nu}{E}\delta_{ij}\delta_{kl} + \frac{1}{2G}(\delta_{ik}\delta_{jl} + \delta_{il}\delta_{jk}), \tag{42}$$

so that Eq. (40) gives,

$$\mathcal{S}^0_{ijkl} = \left(-\frac{\nu}{E} + \chi\eta^2\right)\delta_{kl} + \frac{1}{2G}(\delta_{ik}\delta_{jl} + \delta_{il}\delta_{jk}). \tag{43}$$

The above expression for $\mathcal{S}^0_{ijkl}$ can be further simplified if it is expressed in terms of the corresponding open system elastic constants defined as

$$\nu_0 = \frac{\nu - \chi\eta^2 E}{1 + \chi\eta^2 E}, \quad E_0 = \frac{E}{1 + \chi\eta^2 E}, \quad G_0 = G, \tag{44}$$

so that Eq. (43) becomes,

$$\mathcal{S}^0_{ijkl} = -\frac{\nu_0}{E_0}\delta_{ij}\delta_{kl} + \frac{1}{2G_0}(\delta_{ik}\delta_{jl} + \delta_{il}\delta_{jk}). \tag{45}$$

If the concentration, c, or the coupling parameter, η, are small; then, the open system constants reduce to the standard elastic constants.

2.3.2 Methodology for deriving analytical solutions of a stress-diffusion coupled problem

Consider a body $\mathcal{B}$, with boundary $\partial\mathcal{B}$. Furthermore, let $\partial\mathcal{B}$ be sub-divided into

$$\begin{aligned} \partial\mathcal{B} &= (\partial\mathcal{B})_{m1} \cup (\partial\mathcal{B})_{m2} \\ \partial\mathcal{B} &= (\partial\mathcal{B})_{c1} \cup (\partial\mathcal{B})_{c2} \end{aligned} \tag{46}$$

For the mechanical sub-problem, either a displacement or a force should be applied on the boundaries $(\partial\mathcal{B})_{m1}$ and $(\partial\mathcal{B})_{m2}$, respectively. Similarly for the chemical sub-problem, either a concentration or a flux should be applied on $(\partial\mathcal{B})_{c1}$ and $(\partial\mathcal{B})_{c2}$.

Suppose that the analytical stress solution to the associated uncoupled mechanical problem, represented by (2) and (46)$_1$, is known. Given the modified mechanical balance (41), then the same stress solution for the coupled problem as that for the uncoupled one can be used provided that the modified elastic constants are employed.

Then, the equilibrium value, μ_{eq} (23), can be inferred from the boundary conditions of the coupled problem. For an extensive discussion on the possible cases, the reader is referred to [7]. Finally, the concentration field c_{eq} can be obtained from Eq. (37).

3 Finite element implementation of the coupled formulation

The coupled formulation described in the previous section has been implemented into the finite element code Z-set in a fully coupled way, using the methodology described in [4]. The nodal variables are the concentration c and the displacement $\mathbf{u}$. The tensors $\boldsymbol{\sigma}$ and $\boldsymbol{\epsilon}$, are written in columnar format as:

$$\{\tilde{\sigma}\} = \begin{Bmatrix} \sigma_{11} \\ \sigma_{22} \\ \sigma_{33} \\ \sqrt{2}\sigma_{12} \\ \sqrt{2}\sigma_{23} \\ \sqrt{2}\sigma_{31} \end{Bmatrix}, \quad \{\tilde{\epsilon}\} = \begin{Bmatrix} \epsilon_{11} \\ \epsilon_{22} \\ \epsilon_{33} \\ \sqrt{2}\epsilon_{12} \\ \sqrt{2}\epsilon_{23} \\ \sqrt{2}\epsilon_{31} \end{Bmatrix} \tag{47}$$

The vector and matrix shape functions are defined, respectively, as:

$$\begin{aligned} \{N\} &= \{N_1, N_2, \ldots, N_n\} \\ \left[\tilde{N}\right] &= \begin{bmatrix} N_1 & 0 & N_2 & 0 & \ldots & N_n & 0 \\ 0 & N_1 & 0 & N_2 & \ldots & 0 & N_n \end{bmatrix} \end{aligned} \tag{48}$$

The corresponding 2D gradient operators are:

$$[B] = \begin{bmatrix} \frac{\partial N_1}{\partial x_1} & \cdots & \frac{\partial N_n}{\partial x_1} \\ \frac{\partial N_1}{\partial x_2} & \cdots & \frac{\partial N_n}{\partial x_2} \end{bmatrix}$$

$$\left[\tilde{B}\right] = \begin{bmatrix} \frac{\partial N_1}{\partial x_1} & 0 & \frac{\partial N_2}{\partial x_1} & 0 & \cdots & \frac{\partial N_n}{\partial x_1} & 0 \\ 0 & \frac{\partial N_1}{\partial x_2} & 0 & \frac{\partial N_2}{\partial x_2} & 0 & \cdots & \frac{\partial N_n}{\partial x_2} \\ \frac{1}{\sqrt{(2)}}\frac{\partial N_1}{\partial x_2} & \frac{1}{\sqrt{(2)}}\frac{\partial N_1}{\partial x_1} & \frac{1}{\sqrt{(2)}}\frac{\partial N_2}{\partial x_2} & \frac{1}{\sqrt{(2)}}\frac{\partial N_2}{\partial x_1} & \cdots & \frac{1}{\sqrt{(2)}}\frac{\partial N_n}{\partial x_2} & \frac{1}{\sqrt{(2)}}\frac{\partial N_n}{\partial x_1} \end{bmatrix} \tag{49}$$

The Eq. (2) is multiplied by a test function $\mathbf{v}$ and integrated to obtain the weak form:

$$\int_V (-\boldsymbol{\sigma} : \boldsymbol{\epsilon}(\mathbf{v}) + \mathbf{f} \cdot \mathbf{v})\mathrm{d}V + \int_{\partial V} \mathbf{t} \cdot \mathbf{v} \, \mathrm{d}S = 0 \tag{50}$$

where it is recalled that $\mathbf{t}$ is the traction on the surface ∂V, and $\boldsymbol{\epsilon}(\mathbf{v}) = \frac{1}{2}\left(\nabla \mathbf{v} + \nabla \mathbf{v}^\mathrm{T}\right)$. The virtual test function $\{v\}$ and the physical field $\{u\}$ are discretized using the shape functions N as

$$\{v\} = \left[\tilde{N}\right]\{\hat{v}\}, \quad \{u\} = \left[\tilde{N}\right]\{\hat{u}\} \tag{51}$$

The virtual and real strain fields are:

$$\{\tilde{\epsilon}\}(\{v\}) = \left[\tilde{B}\right]\{\hat{v}\}, \quad \{\tilde{\epsilon}\}(\{u\}) = \left[\tilde{B}\right]\{\hat{u}\} \tag{52}$$

Equation (50) has to hold $\forall \{\hat{v}\}$ and thereby reduces to the discretized mechanical equilibrium residual:

$$\{r_u\} = \int_V (-\{\tilde{\sigma}\}^\mathrm{T}\left[\tilde{B}\right] + \left[\tilde{N}\right]\{f\})\mathrm{d}V + \int_{\partial V} \left[\tilde{N}\right]\{t\} \, \mathrm{d}S \tag{53}$$

The mass balance (1) is multiplied by a test function $c^\star$ and integrated to obtain the weak form:

$$\int_V (\dot{c}\, c^\star - \{j\}\{\nabla w\})\mathrm{d}V + \int_{\partial V} \{j\}\{n\}\, c^\star \, \mathrm{d}S = 0 \tag{54}$$

The virtual and real concentration fields, $c^\star$ and c, are discretized as:

$$c^\star = \{N\}\{\hat{c}^\star\}, \quad c = \{N\}\{\hat{c}\} \tag{55}$$

The Eq. (54) is expressed as the discretized concentration residual as:

$$\{r_c\} = \int_V (\{N\}\{N\}^\mathrm{T}\{\dot{\hat{c}}\} - [B]^\mathrm{T}\{j\})\mathrm{d}V + \int_{\partial V} \{N\}\, j \, \mathrm{d}S, \tag{56}$$

In order to solve the nonlinear sets of equations represented by (53) and (56) with a Newton-Raphson algorithm, a global tangent stiffness matrix, $\mathbf{K}$, is needed. Four terms are identified in the stiffness matrix:

$$[K] = \begin{bmatrix} [K_{uu}] & [K_{uc}] \\ [K_{cu}] & [K_{cc}] \end{bmatrix} \tag{57}$$

with components

$$
[K_{cc}]_{ij} = \frac{\partial \{r_c\}_i}{\partial \hat{c}_j} = \int_V N_i N_j \frac{1}{\Delta t} - B_{ik} \frac{\partial j_k}{\partial \hat{c}_j} \mathrm{d}V
$$

$$
[K_{cu}]_{ij} = \frac{\partial \{r_c\}_i}{\partial \hat{u}_j} = \int_V -B_{ik} \frac{\partial j_k}{\partial \hat{u}_j} \mathrm{d}V
$$

$$
[K_{uu}]_{ij} = \frac{\partial \{r_u\}_i}{\partial \hat{u}_j} = \int_V -\tilde{B}_{ik} \frac{\partial \tilde{\sigma}_k}{\partial \hat{u}_j} \mathrm{d}V
$$

$$
[K_{uc}]_{ij} = \frac{\partial \{r_u\}_i}{\partial \hat{c}_j} = \int_V -\tilde{B}_{ik} \frac{\partial \tilde{\sigma}_k}{\partial \hat{c}_j} \mathrm{d}V
$$

(58)

It can be shown that the stiffness matrix derivatives need to be consistent with the choice of free energy made in Sect. 2.2.2 :

$$
\frac{\partial j_k}{\partial \hat{c}_j} = -N_j \frac{\partial L}{\partial c} \frac{\partial \mu}{\partial x_k} - L N_j \frac{\partial^3 \psi}{\partial c^3} \frac{\partial c}{\partial x_k} - L \frac{\partial^2 \psi}{\partial c^2} \frac{\partial N_j}{\partial x_k}
$$

$$
\frac{\partial j_k}{\partial \hat{u}_j} = 0
$$

$$
\frac{\partial \tilde{\sigma}_k}{\partial \hat{u}_j} = \left[\frac{\partial^2 \psi}{\partial \boldsymbol{\epsilon} \partial \boldsymbol{\epsilon}} \right]_{ki} \tilde{B}_{ij}
$$

$$
\frac{\partial \tilde{\sigma}_k}{\partial \hat{c}_j} = \left[\frac{\partial^2 \psi}{\partial c \partial \boldsymbol{\epsilon}} \right]_k N_j
$$

(59)

where:

$$
\frac{\partial \mu}{\partial x_k} = \frac{\partial^2 \psi}{\partial c^2} \frac{\partial c}{\partial x_k} - H_{mn} \frac{\partial^2 \psi}{\partial \epsilon_{mn} \partial \epsilon_{pq}} \frac{\partial \epsilon_{pq}}{\partial x_k}
$$

(60)

Concerning local implicit integration of the resulting equations, classical procedures are used in the Z-set code following [4,21]. In the above equation, and in the calculation of the flux (33), the gradient of the total strain tensor is needed. To avoid the use of particular elements, the strain is extrapolated from the Gauss points to the nodes and its gradient is computed with the use of the derivatives of the shape functions. This method is the same as the one used by Thomas and Chopin [22] and Abrivard et al [1].

4 Analytical and numerical solutions to some boundary values problems

In this section, the steady-state concentration field in three examples is determined solving the coupled problems both numerically and analytically. The analytic equilibrium solution is obtained by solving directly the coupled equation driving the system for the first example, and the procedure described in the Sect. 2.3 for the other two.

4.1 Rotating disc

The first problem is a disc with an initial homogeneous vacancy concentration, c_0, which is rotating at a constant velocity, ω. Only elasticity is taken into account. An illustration of the rotating disc is given in Fig. 1. The boundary conditions are chosen so that an exact solution can be found in an axisymmetric setting. The vanishing flux on top and bottom surfaces ($z = 0$ and $z = h$) enforces a quasi-1D character (radial only) to the solution. The numerical parameters chosen for the calculations are given in Table 1. The dimension of the disc is $d = 400$ mm and $h = 10$ mm. The parameter χ from Eq. (36) is evaluated for $c = c_0$ in the analytical treatment: the boundary condition on the external surface (at $r = d$) represents *a chemical reservoir*, where a constant concentration is maintained.

From Eqs. (1) and (17), it can be seen that the rate of change of the concentration is given by:

$$
\dot{c} = -\operatorname{div} \mathbf{j} = \operatorname{div}(L \nabla \mu) = 0.
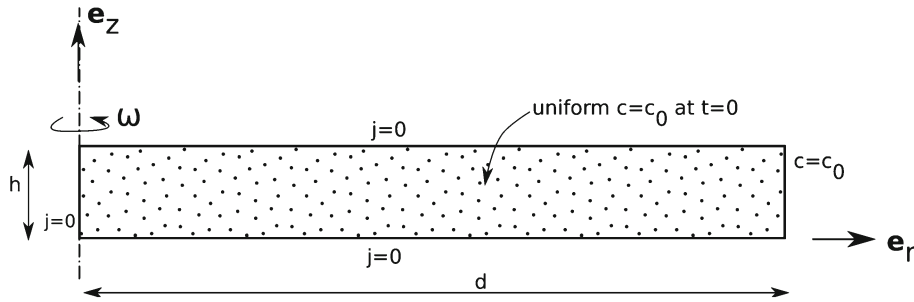$$

(61)

Fig. 1 Definition of the rotating disc set-up: geometry, boundary conditions and mechanical loading

Table 1 Simulation parameters used for the rotating disc problem, nickel

c_0	T	v_a	E	ν	η	ω
[.]	[K]	[mm^3 mol^{-1}]	[GPa]	[.]	[.]	[rad s^{-1}]
1×10^{-4}	900	$6, 6 \times 10^3$	200	0.34	-0.05	$2, 09 \times 10^3$

Furthermore, the stress state at a generic radial position, r, of the disc can be expressed in polar coordinates in terms of its outer radius, d, its mass density, ρ, the angular velocity ω, and open system Poisson's ratio, v_0,

$$\sigma_{rr} = \frac{(3 + v_0)}{8} \rho \omega^2 \left(d^2 - r^2\right),\tag{62}$$

and

$$\sigma_{\theta\theta} = \frac{\rho\omega^2}{8} \left[(3 + v_0)d^2 - (1 + 3v_0)r^2\right].\tag{63}$$

The corresponding trace of the stress tensor is then,

$$\mathrm{tr}(\boldsymbol{\sigma}) = \frac{\rho\omega^2}{4} \left[(3 + v_0)\, d^2 - 2\, r^2(1 + v_0)\right].\tag{64}$$

The equilibrium solution to the boundary value problem can be found by combining Eqs. (61) with (33) and (64), i.e.

$$0 = \mathrm{div}\,(L\,\nabla\mu) = D\frac{\partial^2 c}{\partial r^2} + D\left(\frac{\Delta v\rho\omega^2(1 + v_0)}{3R\,T}r + \frac{1}{r}\right)\frac{\partial c}{\partial r} + 2D\frac{\Delta v\rho\omega^2(1 + v_0)}{3R\,T}c.\tag{65}$$

Leading to the following differential equation:

$$\frac{\partial^2 c}{\partial r^2} + \left(Ar + \frac{1}{r}\right)\frac{\partial c}{\partial r} + 2\,A\,c = 0.\tag{66}$$

with

$$A = \frac{\Delta v\rho\omega^2(1 + v_0)}{3RT},\tag{67}$$

A general solution for Eq. (66) is,

$$c(r) = C_1 \exp\left(-\frac{1}{2}Ar^2\right) + C_2 \exp\left(-\frac{1}{2}Ar^2\right) \int_1^\infty \frac{\exp(\frac{1}{2}Ar^2 x)}{x}\mathrm{d}x,\tag{68}$$

where C_1 and C_2 are two integration constants to be determined from the boundary conditions shown on Fig. 1, that is, $j_r = 0$ at r=0, and a prescribed concentration, $c = c_0$, on the external surface at $r = d$. Thus

$$j_r(0) = \frac{\partial\mu}{\partial r}(0) = \frac{\partial c}{\partial r}(0) = 0, \quad \text{and} \quad c(d) = c_0.\tag{69}$$

and the solution given by Eq. (68) becomes:

$$c(r) = c_0 \exp\left(\frac{1}{2}A\left(d^2 - r^2\right)\right). \tag{70}$$

The equilibrium diffusion potential, μ_{eq}, can be obtained from Eqs. (34) and Eq. (64),

$$\mu_{eq} = \frac{RT}{v_a}\ln c_0 + \frac{E_f}{v_a} + \frac{\Delta v}{v_a}\rho\,\omega^2\,\frac{v_0 - 1}{12}\,d^2. \tag{71}$$

However, for the particular example of interest here, the value of μ_{eq} is actually known *a priori* at $r = d$ since both the concentration and stresses are known at that free boundary. In this case, it would also have been possible to calculate μ_{eq} from Eq. (23) using the boundary condition and analytical stress at $r = d$, and directly use it in Eq. (34) to retrieve Eq. (70).

The numerical simulation recovers exactly the analytical coupled solution of this problem, as shown by the profile of concentration given on Fig. 2. For this example, a reduction of 17 % of the initial concentration at $r = 0\,(\eta = -0.05)$, and 1.7 % for $\eta = -5\times 10^{-3}$ is found. Note that the stress σ_{rr} is approximately 1,000 MPa, which would in reality induce plasticity. The value of η is critical, and also subject of discussion since various different parameters can be found in the literature, even with positive signs in aluminium (e.g. see [23] and [8]).

4.2 Vacancy diffusion around the core of an edge dislocation

Consider an edge dislocation of Burgers vector b, located at a point with coordinates $(x, y) = (0, 0)$ in an infinite plate with an initial homogeneous vacancy concentration, $c_{ref} = c_0$. The edge dislocation was introduced in the finite element model by imposing a shear eigenstrain in a thin semi-infinite strip of thickness h, with magnitude $-b/h$, and only elasticity is taken into account. In order to determine the equilibrium vacancy concentration state in the system, the following boundary conditions are imposed: a vanishing flux is assumed on the dislocation core boundary (with a radius equal to $2b$), and a constant concentration $c = c_0$, on the far-field boundaries, i.e. the dislocation is considered to be in a *chemical reservoir*. The set-up is illustrated on Fig. 3.

In the analytical solution, the parameter χ from Eq. (36) was determined for $c = c_0$ using the chemical reservoir boundary conditions. The stress field in Cartesian coordinates around the edge dislocation takes the form of the Hirth and Lothe [11] solution, albeit with the open system elastic constants instead of the standard ones. Here,

$$\sigma_{xx} = -\frac{G_0 b}{2\pi(1 - v_0)}\frac{y\left(3x^2 + y^2\right)}{\left(x^2 + y^2\right)^2}, \tag{72}$$
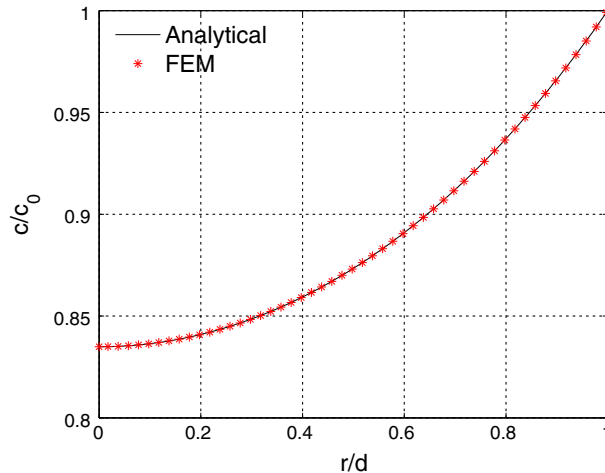

Fig. 2 Concentration profile in the rotating disc, normalised by c_0, as a function of the normalised distance from the axisymmetric axis

$$\sigma_{yy} = \frac{G_0 b}{2\pi(1-\nu_0)} \frac{y(x^2-y^2)}{(x^2+y^2)^2}, \tag{73}$$

$$\sigma_{zz} = \nu_0(\sigma_{xx}+\sigma_{yy}), \tag{74}$$

$$\sigma_{xy} = \frac{G_0 b}{2\pi(1-\nu_0)} \frac{x(x^2-y^2)}{(x^2+y^2)^2} \tag{75}$$

The analytical vacancy concentration solution can be approximated with the linearised Eq. (37):

$$c_{eq} = c_0 - \chi\eta(1+\nu_0)\frac{G_o b}{\pi(1-\nu_0)} \frac{x^2 y + y^3}{(x^2+y^2)^2} \tag{76}$$

The parameters used to obtain the numerical and analytical results are given in Table 2. The vacancy formation energy is close to the value given in [20], from which c_0 is obtained. Other values are taken from [10] for aluminium. The analytical and numerical results are given in Figs. 4 and 5.

The evolution of the normalised steady-state vacancy concentration profiles around the dislocation core (along y/b at $x=0$) obtained both analytically and numerically are depicted in Fig. 4, where an excellent correlation is found even at a location as close as $5b$ from the centre of the dislocation core. The corresponding contour plots of the steady-state normalised vacancy concentration around the edge dislocation core is given in Fig. 5. As expected, vacancies tend to relieve the hydrostatic pressure around the dislocation core by migrating from the tensile regions to the compressive ones, a classical result given by Hirth and Lothe [11]. Finally, it is possible to analytically obtain the effect of the vacancy concentration on the stress. If P_{ref} and P are the pressure around the dislocation core, without and with vacancies respectively, then:

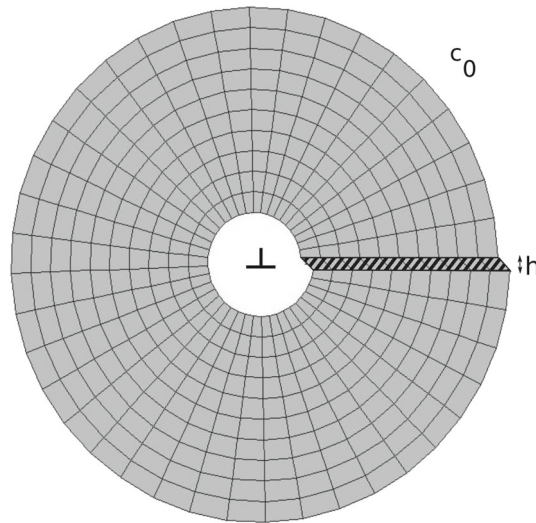$$\frac{P}{P_{ref}} = \frac{(1+\nu_0)(1-\nu)}{(1+\nu)(1-\nu_0)} \tag{77}$$

Fig. 3 Model of the edge dislocation problem (deformed configuration, zoomed on the core): an eigenstrain $\epsilon_{12}^\star = -b/h$ is imposed in the stripped zone, and a cut-out of radius 2b is made to exclude the core, with a vanishing flux boundary condition. A concentration c_0 is imposed on the far-field boundaries

Table 2 Parameters used to simulate vacancy diffusion around an edge dislocation

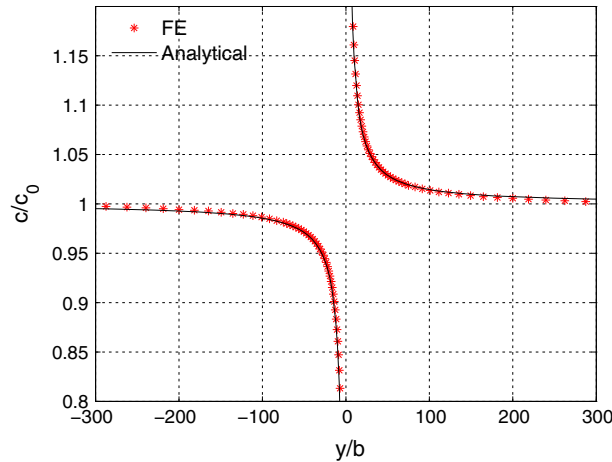| h	c_0	T	v_a	η	E	ν
[nm]	[.]	[K]	[m^3 mol^{-1}]	[.]	GPa	[.]
0.5	10^{-4}	700	10^{-5}	-0.05	70	0.34

Fig. 4 Variations of the normalised steady-state vacancy concentration profile along y/b at $x = 0$, obtained both analytically and numerically
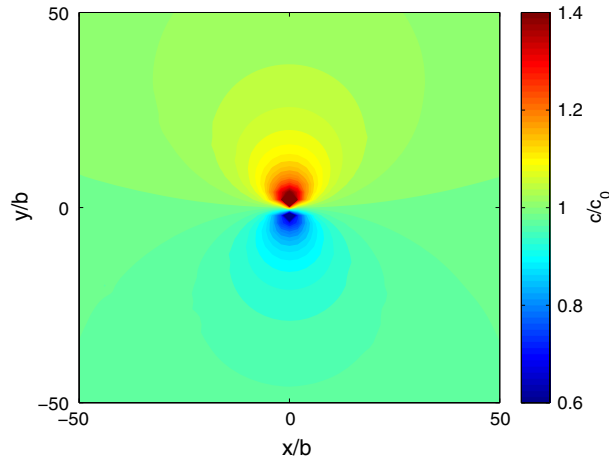

Fig. 5 Contour plot of the numerically obtained equilibrium vacancy concentration distribution normalised by c_0. The vacancies tend to relieve the hydrostatic pressure around the dislocation core by migrating from the tensile regions to the compression ones

which is independent of position. For instance, $\frac{P}{P_{\text{ref}}} = 0.9991$ and 0.9242 for $c_0 = 10^{-3}$ and $c_0 = 10^{-1}$, respectively. Even considering the typical concentrations values encountered at homologous temperature, the influence of vacancies on the stress state is negligible in most cases.

4.3 Perforated plate subject to a far-field tensile stress

The last example concerns the analysis of an infinite plate with a centred hole of radius $R_h = 1 \mu m$ subject to a far-field tensile stress σ_∞. First, a pure elastic case will be discussed, then an elastic perfectly plastic model with yield stress σ_y will be considered. The far-field stress σ_∞ is applied along the $x-$axis (see Fig. 6). The steady-state solution to the coupled diffusion elasticity problem in polar coordinates (r, θ)—θ being the angle with respect to the x axis—is given by the classical one in terms of the open system Poisson's ratio, v_0, namely

$$\sigma_{rr} = \frac{\sigma_\infty}{2}\left(1 - \left(\frac{R_h}{r}\right)^2\right) + \frac{\sigma_\infty}{2}\left(1 + 3\left(\frac{R_h}{r}\right)^4 - 4\left(\frac{R_h}{r}\right)^2\right)\cos(2\theta),$$

$$\sigma_{\theta\theta} = \frac{\sigma_\infty}{2}\left(1 + \left(\frac{R_h}{r}\right)^2\right) - \frac{\sigma_\infty}{2}\left(1 + 3\left(\frac{R_h}{r}\right)^4\right)\cos(2\theta),$$

$$\sigma_{zz} = \sigma_\infty \nu_0\left(1 - 2\left(\frac{R_h}{r}\right)^2\cos(2\theta)\right),$$

$$\sigma_{r\theta} = -\frac{\sigma^\infty}{2}\left(1 - 3\left(\frac{R_h}{r}\right)^4 + 2\left(\frac{a}{r}\right)^2\right)\sin(2\theta).$$

(78)

Then, the corresponding trace of the stress tensor is

$$\text{tr}(\boldsymbol{\sigma}) = (1 + \nu_0)\,\sigma_\infty\left(1 - 2\left(\frac{R_h}{r}\right)^2\cos(2\theta)\right).$$

(79)

The far-field stress was chosen so that the plate deforms uniaxially along the x-axis at the far field by 0.2 %. The parameters used in the analytical and numerical calculations are given in Table 3 for aluminium. The analytical vacancy concentration field is obtained from Eq. (37) using the expression for the trace of the stress tensor, Eq. (79). The value of the parameter χ is taken for $c = c_0$, again, due to the chemical reservoir type of the boundary condition.

A contour plot of the numerically obtained distribution of the vacancy concentration at equilibrium within the plate, normalised by c_0, is shown for the elastic case in Fig. 6. The stress concentration factors, defined as the ratio $\sigma_{yy}/\sigma_\infty$ at the inner hole boundary are known to be -1 and 3 for $\theta = 0°$ and 90°, respectively. As a result of these stress concentration effects, vacancies redistribute around the hole, see Fig. 6. Red regions ($\theta = 0°$) exhibit a concentration above the initial value and the blue ones ($\theta = 90°$) a decrease relative to c_0. The hole radius being small, the stress gradients act in this case as a strong driving force for the vacancy fluxes.

To illustrate the extended theory, a perfectly plastic behaviour is now incorporated in the model. Here, plasticity is expected to relax the stresses locally, leading to smaller stress gradients and hence affecting the
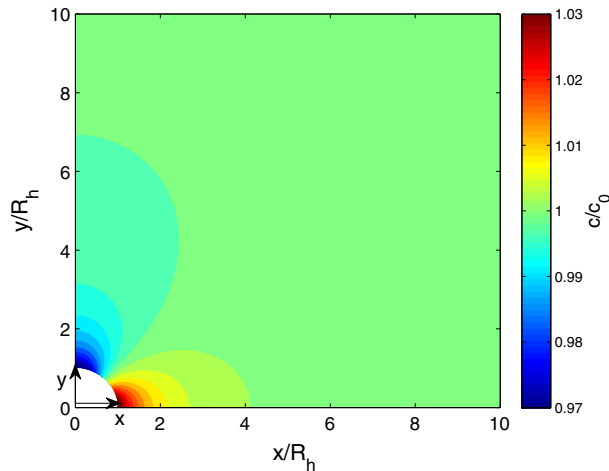

Fig. 6 Contour plot of the numerically obtained equilibrium vacancy concentration distribution normalised by c_0, obtained numerically in the elastic case, around a hole in a plate

Table 3 Simulation parameters used in the infinite plate with a centred hole case

c_0	T	ν_a	E	σ_y	ν	η	R_h
[.]	[K]	[m^3.mol^{-1}]	[GPa]	[MPa]	[.]	[.]	[μm]
10^{-4}	700	10^{-5}	70	200	0.34	-0.05	1.

fluxes and the equilibrium state. The trace of the stress distribution around the hole ($r = R_h$) at different angles θ, is given in Fig. 7 for various initial concentrations. The coupled open system elastic constants influence the stresses only for high vacancy concentrations, the term χ being negligible in Eq. (44) when $c = 10^{-4}$. When the hypothesis $c \ll 1$ made in the analytical developments is verified, the FE solution is indistinguishable from the analytical solution. However, this is no longer true when $c = 0.1$, explaining the small discrepancy observed between the analytical and FE solutions. When c is large, the analytical solution tends to underestimate the stress compared to the FE solution. The reduction of the stress gradient in the plastic case is clearly visible for $\theta > 40°$.

The results in Fig. 8 are shown in terms of the normalised vacancy concentration along the surface of the hole. Also shown are the concentration profiles predicted analytically using both the standard elastic constants and the open system elastic ones (denoted 'Coupled Analytical' in the figure), and the numerically obtained results (FE) in the elastic and plastic cases. In the plastic case, the methodology presented in Sect. 2.3 is applied. The stress field calculated numerically is used to compute the concentration field analytically, using Eq. (37), and an adequate agreement is found with the coupled FE solution and the semi-analytical one.

Finally, in the plastic case, the plate is loaded as before until equilibrium is reached, and then unloaded. Due to the plastic deformation that has occurred on the top side of the hole, the unloaded configuration is not homogeneously deformed. This leads to residual stresses upon unloading giving a non-uniform distribution of vacancies in the unloaded configuration. This is visible in Fig. 9 numerical results.
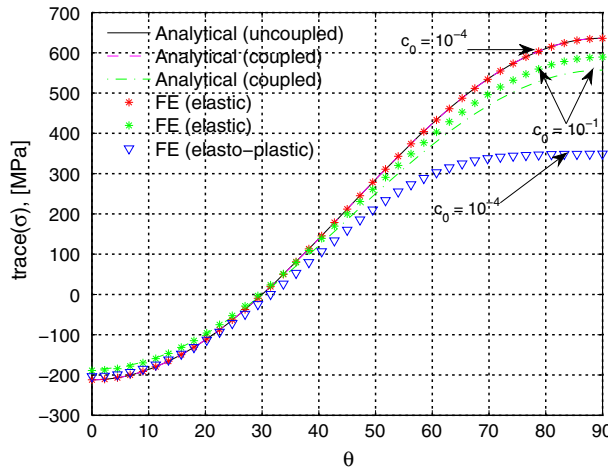

Fig. 7 Variation of the trace of the stress tensor around the hole for two different values of initial vacancy concentration, without and with the effect of the open system (ie, coupled) elastic constants. The effect of the concentration on the stress is noticeable for high concentrations
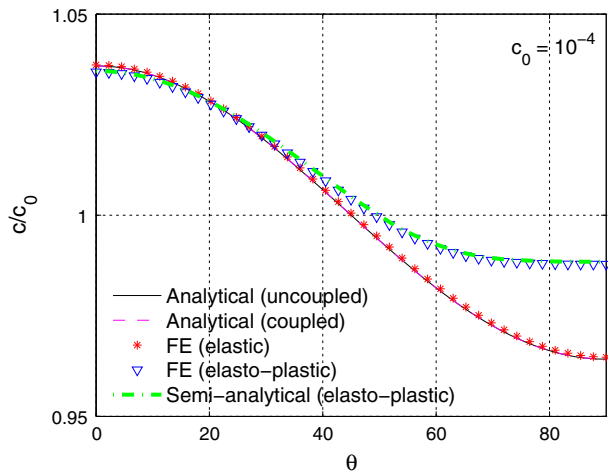

Fig. 8 Concentration profile around the hole of a plate loaded uni-axially, obtained analytically and numerically for the elastic case, and numerically for the elasto-plastic one
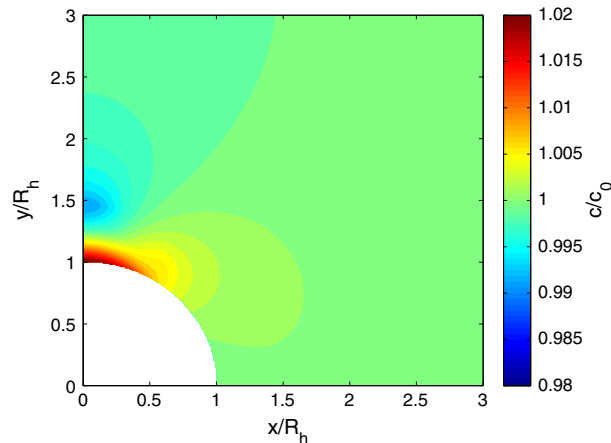
Fig. 9 Residual distribution of vacancies obtained after unloading in the plastic case. Due to the stress concentration factor on the top of the hole, plastic deformation heterogeneities upon unloading give rise to residual stresses that lead, in turn, to vacancy redistribution

5 Summary

A thermodynamically consistent diffusion-stress coupling framework has been developed for elasto-viscoplastic solids. To obtain the equilibrium stress and composition fields, a coupled solution of the equations governing mechanical and chemical equilibrium is normally required. However, it is possible to obtain both fields by only solving a modified mechanical equilibrium equation, in which modified elastic constants account implicitly for the chemical equilibrium. First introduced by Cahn and Larché for an elastic solid, they are called open system elastic constants, derived at constant diffusion potential, the procedure being similar to the one giving adiabatic compliance instead of isothermal one. It has been shown that, in presence of plasticity, these derivations are still valid, and enable an analytical solution of the concentration field to be obtained knowing the numerical stress field. Three coupled problems have been treated analytically and numerically to illustrate the efficiency of this method.

The coupled diffusion-stress formulation has been implemented in a finite element framework in a fully coupled way. The resulting numerical predictions of different problems capture the main features of the coupled phenomena predicted analytically. When the concentration is very small, the values of the open system constants are close to the conventional values, and the concentration field can be calculated from the stress field obtained using either set of constants. However, when the concentration is relatively high, it becomes necessary to use the open system compliances for the simulations to remain in agreement with the analytical solutions. Finally, if the concentration is not negligible compared to 1, a discrepancy between the FEM and analytical solutions arises.

The role of plasticity on the local relaxation of the stress state and its effects on the corresponding equilibrium concentration field has been illustrated in a simple example. The plasticity model was limited to a perfect one in the simulations, although the proposed theory accounts for hardening.

The study of the redistribution of vacancies around an edge dislocation is of interest, amongst other applications, for the modelling of dislocation climb assisted by diffusion, by providing an explicit framework to determine the local vacancy concentration distribution around the dislocation core. Accounting for the effects of stress on point defect diffusion is also relevant for modelling the formation of stable vacancy clusters in irradiated materials. In this case, the concentration of vacancies is high, which has been shown to have a non-negligible effect on the open system constants. Recent work in this area by [14], based on phase-field techniques, neglected the effects of stress so that no effect of applied load could be accounted for on void growth. If omitted, stress gradients are unable to affect the vacancy fluxes responsible for altering the shape of the void and their kinetics. The framework presented here provides the necessary analytical tools to pursue such goal.

Appendix: Derivation of open system elastic constants

Contrary to the approach presented in [7], the derivation is here based on the enthalpy, $h(c, \boldsymbol{\sigma}, \mathrm{p}, \boldsymbol{\alpha})$, for simplicity. The diffusion potential and the strain tensor components can be expressed as

$$\mu = \left.\frac{\partial h}{\partial c}\right|_{\sigma_{ij}}, \quad \text{and} \quad -\epsilon_{ij} = \left.\frac{\partial h}{\partial \sigma_{ij}}\right|_{c}. \tag{80}$$

From Eq. (80), the so-called Maxwell relation can be obtained:

$$\left.\frac{\partial \mu}{\partial \sigma_{kl}}\right|_{c} = \frac{\partial^2 h}{\partial \sigma_{kl} \partial c} = \frac{\partial^2 h}{\partial c \partial \sigma_{kl}} = -\left.\frac{\partial \epsilon_{kl}}{\partial c}\right|_{\sigma_{kl}} \tag{81}$$

Recalling that the strain can be partitioned as,

$$\boldsymbol{\epsilon} = \boldsymbol{\epsilon}^{\mathrm{e}} + \mathbf{H}(c - c_{\mathrm{ref}}) + \boldsymbol{\epsilon}^{\star}_{\mathrm{ref}} + \boldsymbol{\epsilon}^{\mathrm{p}} \tag{82}$$

and expressing the elastic strain tensor in terms of the stress tensor and the compliance tensor, $\mathcal{S} = \mathcal{C}^{-1}$, yields,

$$\boldsymbol{\epsilon} = \mathcal{S} : \boldsymbol{\sigma} + \mathbf{H}(c - c_{\mathrm{ref}}) + \boldsymbol{\epsilon}^{\star}_{\mathrm{ref}} + \boldsymbol{\epsilon}^{\mathrm{p}} \tag{83}$$

Differentiating the strain components at fixed internal variables,

$$\mathrm{d}\epsilon_{ij} = \left.\frac{\partial \epsilon_{ij}}{\partial \sigma_{kl}}\right|_{c} \mathrm{d}\sigma_{kl} + \left.\frac{\partial \epsilon_{ij}}{\partial c}\right|_{\sigma_{ij}} dc, \tag{84}$$

and the diffusion potential, μ,

$$\mathrm{d}\mu = \left.\frac{\partial \mu}{\partial \sigma_{kl}}\right|_{c} \mathrm{d}\sigma_{kl} + \left.\frac{\partial \mu}{\partial c}\right|_{\sigma_{ij}} dc, \tag{85}$$

solving for dc in Eq. (85),

$$dc = \left(\mathrm{d}\mu - \left.\frac{\partial \mu}{\partial \sigma_{kl}}\right|_{c} \mathrm{d}\sigma_{kl}\right) \left(\left.\frac{\partial \mu}{\partial c}\right|_{\sigma_{ij}}\right)^{-1}, \tag{86}$$

and substituting the Maxwell relation into Eq. (86) leaves,

$$dc = \left(\mathrm{d}\mu + \left.\frac{\partial \epsilon_{kl}}{\partial c}\right|_{\sigma_{kl}} \mathrm{d}\sigma_{kl}\right) \left(\left.\frac{\partial \mu}{\partial c}\right|_{\sigma_{ij}}\right)^{-1}. \tag{87}$$

Finally, substituting Eq. (87) into Eq. (84) and re-arranging yields,

$$\mathrm{d}\epsilon_{ij} = \left(\left.\frac{\partial \epsilon_{ij}}{\partial \sigma_{kl}}\right|_{c} + \left.\frac{\partial \epsilon_{ij}}{\partial c}\right|_{\sigma_{ij}} \left.\frac{\partial \epsilon_{kl}}{\partial c}\right|_{\sigma_{kl}} \left(\left.\frac{\partial \mu}{\partial c}\right|_{\sigma_{ij}}\right)^{-1}\right) \mathrm{d}\sigma_{kl} + \left.\frac{\partial \epsilon_{ij}}{\partial c}\right|_{\sigma_{ij}} \mathrm{d}\mu. \tag{88}$$

Cahn and Larché [6] defined the term in brackets in Eq. (88) as the *open system compliance* at a constant potential μ, or $\mathcal{S}^{0}_{ijkl}$. Thus,

$$\mathcal{S}^{0}_{ijkl} = \left.\frac{\partial \epsilon_{ij}}{\partial \sigma_{kl}}\right|_{\mu} = \left.\frac{\partial \epsilon_{ij}}{\partial \sigma_{kl}}\right|_{c} + \left(\left.\frac{\partial \epsilon_{ij}}{\partial c}\right|_{\sigma_{ij}} \left.\frac{\partial \epsilon_{kl}}{\partial c}\right|_{\sigma_{kl}}\right) \left(\left.\frac{\partial \mu}{\partial c}\right|_{\sigma_{ij}}\right)^{-1}. \tag{89}$$

The expression for the open system compliance defined above can be obtained by recalling the following relations,

$$\left.\frac{\partial \epsilon_{ij}}{\partial \sigma_{kl}}\right|_{c} = \mathcal{S}_{ijkl}, \quad \text{and} \quad \left.\frac{\partial \epsilon_{ij}}{\partial c}\right|_{\sigma_{kl}} = H_{ij}. \tag{90}$$

Then, Eq. (40) is retrieved.

References

1. Abrivard, G., Busso, E.P., Forest, S., Appolaire, B.: Phase field modelling of grain boundary motion driven by curvature and stored energy gradients. part I: theory and numerical implementation. Philos. Mag. **92**(28-30), 3618–3642 (2012)
2. Anand, L.: A thermo-mechanically-coupled theory accounting for hydrogen diffusion and large elastic-viscoplastic deformations of metals. Int. J. Solids Struct. **48**(6), 962–971 (2011)
3. Ballufi, R.W., Allen, S.M., Carter, W.C.: Kinematics of Materials. Wiley, New York (2005)
4. Besson, J., Cailletaud, G., Chaboche, J.L., Forest, S.: Nonlinear Mechanics of Materials. Springer, Berlin (2010)
5. Cahn, J.: Thermodynamic aspects of cottrell atmospheres. Philos. Mag. **0**, 1–6 (2013)
6. Cahn, J., Larché, F.: A linear theory of thermochemical equilibrium of solids under stress. Acta Metall. **21**, 1051–1063 (1973)
7. Cahn, J., Larché, F.: The interactions of composition and stress in crystalline solids. Acta Metall. **33**, 331–357 (1985)
8. Clouet, E.: The vacancyedge dislocation interaction in fcc metals: a comparison between atomic simulations and elasticity theory. Acta Mater. **54**(13), 3543–3552 (2006)
9. Cottrell, A.: An Introduction to Metallurgy. 2nd edn. Edward Arnold, London (1975)
10. Frost, H., Ashby, F.: Deformation-mechanism maps: the plasticity and creep of metals and ceramics. Pergamon Press, Oxford (1982)
11. Hirth, J.P., Lothe, J.: Theory of Dislocation. 2nd edn. Wiley, New York (1982)
12. Lemaitre, J., Chaboche, J.: Mechanics of Solid Materials. Cambridge University Press, Cambridge (1994)
13. Maugin, G.A.: On the thermomechanics of continuous media with diffusion and/or weak nonlocality. Arch. Appl. Mech. **75**(10-12), 723–738 (2006)
14. Millett, P.C., El-Azab, A., Rokkam, S., Tonks, M., Wolf, D.: Phase-field simulation of irradiated metals part I: void kinetics. Comput. Mater. Sci. **50**, 949–959 (2011)
15. Paukshto, M.: Diffusion-induced stresses in solids. Int. J. Fract. **97**(1-4), 227–236 (1999)
16. Pavlina, V., Podstrigach, Y.: Residual stresses due to diffusion in an elastic homogeneous plate Sov.. Mater. Sci. **4**(4), 279–283 (1971). doi:10.1007/BF00722614
17. Podstrigach, Y., Pavlina, V.: Differential equations of thermodynamic processes in n-component solid solutions Sov.. Mater. Sci. **1**(4), 259–264 (1966). doi:10.1007/BF00714880
18. Podstrigach, Y., Shevchuk, P.: Diffusion phenomena and stress relaxation in the vicinity of a spherical void Sov.. Mater. Sci. **4**(2), 140–145 (1969). doi:10.1007/BF00715566
19. Rauh, H, Simon, D: Diffusion process of point-defects in the stress-field of edge dislocations. Phys. Status Solidi **46**(2), 499–510 (1978)
20. Shewmon, P.: Diffusion in Solids. Wiley, New York (1989)
21. Simo, J., Hughes, T.: Computational Inelasticity. Springer, Berlin (1997)
22. Thomas, J., Chopin, C.: Modeling of coupled deformation-diffusion in non-porous solids. Int. J. Eng. Sci. **37**(1), 1–24 (1999)
23. Was, G.S.: Fundamentals of Radiation Materials Sciences. Springer, Berlin (2007)
24. Xuan, F.Z., Shao, S.S., Wang, Z., Tu, S.T.: Coupling effects of chemical stresses and external mechanical stresses on diffusion. J. Phys. D Appl. Phys. **42**(1), 015401 (2009)
25. Yang, F.: Interaction between diffusion and chemical stresses. Mater. Sci. Eng. A **409**, 153–159 (2005)